FEATURES OF JET PLASMA BEHAVIOUR IN TWO DIFFERENT DIVERTOR CONFIGURATIONS

The JET Team[1]
(presented by J Jacquinot)

JET Joint Undertaking,
Abingdon, Oxfordshire,
United Kingdom.

Abstract

Two pumped divertors have been installed and tested in JET under ITER relevant conditions. A closed divertor is found to increase the particle and impurity exhaust rate in agreement with code modelling. Excellent power handling is demonstrated allowing high current discharges with record stored energy (15 MJ) and quasi steady-state discharges with high fusion triple product (4×10^{20} m^{-3} s keV). The ITERH93-P confinement scaling law is confirmed over a broad range and a more favourable β scaling is found. No hysteresis is found in the H-mode power threshold. A data base of highly radiating discharges including impurity seeding describes the relationship between radiated power, impurity concentration and density.

First results of high performance with optimised magnetic shear are presented. Strong internal confinement barriers develop despite the relatively small input of toroidal momentum and particle fuelling from ICRH and NBI.

1. INTRODUCTION - JET, A FLEXIBLE FACILITY

The JET Joint Undertaking is an organisation involving the participation of 15 European countries with central funding from EURATOM. The JET machine [1] was designed with the essential objectives of obtaining and studying plasmas in conditions and dimensions approaching those required in a fusion power plant. In order to pursue new objectives, JET has been extended to the end of 1999 to make essential contributions to a viable divertor concept for ITER and carry out D/T experiments in an ITER-like configuration.

JET has considerable flexibility that allows the study of many different modes of operation. It can match ITER geometry and dimensionless parameters (except the normalised Larmor radius, ρ^*) and can study the effect of large variations around the ITER values. JET has operated at 6 MA in H-mode [2]. D/T plasmas were studied for the first time in 1991 [3]. In preparing for the forthcoming D/T phase (DTE1) to be carried out in early 1997, a closed circuit gas handling system is being commissioned with 3 g of tritium which will be increased to 10 g for the experiments. Remote handling of in-vessel components is an integral part of the programme and will be used for a divertor target exchange after DTE1.

JET has a coherent divertor programme which includes divertor model validation. The main thrust of the programme is to operate successively a series of single-null divertor configurations (Section 2) with increasing "closure", ie the fraction of recycled neutrals escaping from the divertor region is increasingly smaller. Retaining the neutrals in the divertor region leads to a higher density and lower temperature divertor plasma for a given scrape-off layer (SOL) power and

[1] See Appendix

mid-plane separatrix density. The pumping in the divertor region is therefore made easier. Target sputtering could be reduced (unless chemical sputtering is dominant) and the retention of impurities could be enhanced [4]. However, ELMs (Edge Localised Modes) could defeat some of the favourable features of closed divertors by producing strong interactions with plasma facing components outside the target plates.

The divertor programme includes the successive testing of three pumped divertors between 1994 and 1998 with the following sequence :

- in 1994-1995, Mk I: an open divertor requiring sweeping the heat load in the divertor region;
- in 1996-1997, Mk IIA: a moderately closed divertor with a large wetted area. This divertor can accommodate up to 40MW for 8s without sweeping. In Mk IIA, operation is possible on both the horizontal and vertical target plates. Mk IIA is compared with Mk I in Fig. 1; and
- in 1997-1998, Mk II GB: a closed gas box divertor configuration to be installed by remote handling after DTE1.

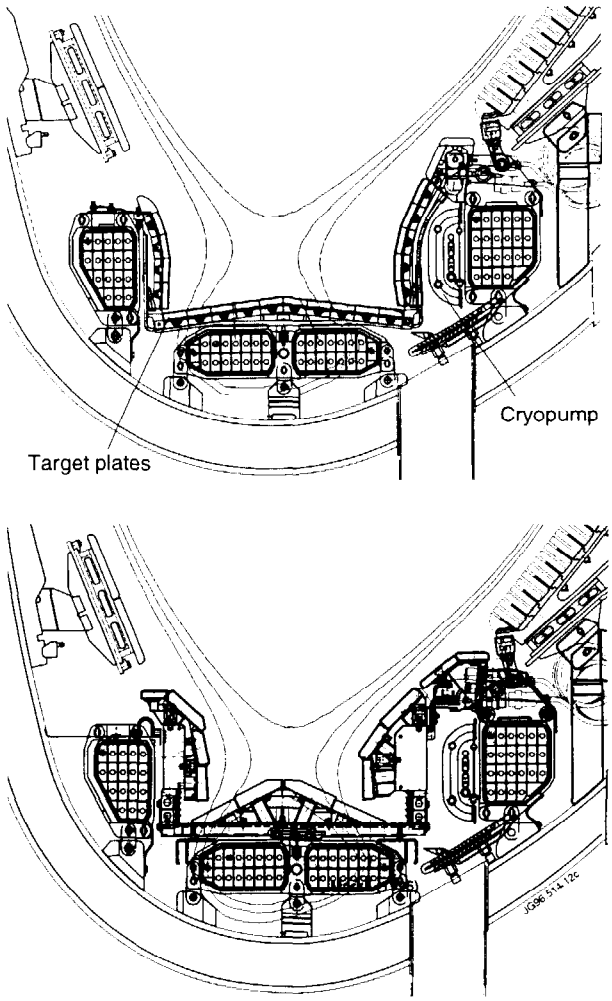

Fig.1 A view of the poloidal cross-section of the Mk I (top) and Mk IIA (bottom) pumped divertors.

Parameter	
Plasma minor radius, a (m)	0.95
Plasma half height, b (m)	1.75
Plasma major radius, geometrical centre, R_0 (m)	2.85
Plasma Volume (m^3)	85
Plasma aspect ratio, R_0/a	3.0
Plasma elongation, b/a	1.85
Toroidal magnetic field (at R_0), $B_{TO}(T)$	3.6
Flat top pulse length, t(s)	10 to 25
Plasma current, I_p (MA)	6.0
Transformer flux, f (Wb)	42
Neutral Beam power at 80 keV and 140 keV, (MW)	21
Ion Cyclotron power at 25 to 55 MHz, (MW)	17
Lower Hybrid power at 3.7 GHz, (MW)	7

TABLE I: JET parameters for Mk I and Mk II divertor experiments

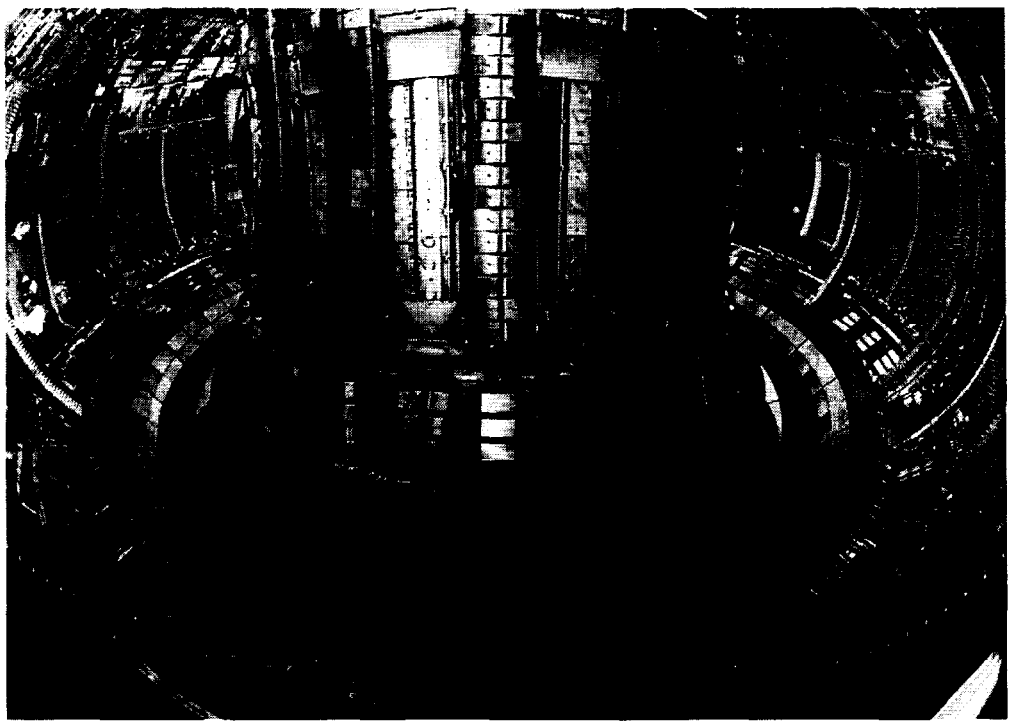

Fig.2 The interior of the modified JET in 1996 showing several important in-vessel components: four ICRH antennae each on the right and left, adjacent lower hybrid launcher on the right, a part of the saddle coils on the inner wall and the Mk IIA divertor on the floor.

The parameters of the JET tokamak are given in Table I. A view of the in-vessel components of JET at the restart of operation in 1996 is given in Fig.2 where some of the components such as the divertor target plates, ion cyclotron

resonance heating (ICRH) antennas and lower hybrid current drive (LHCD) launcher can be seen. The core and divertor plasma parameters are measured with an extensive set of instruments [5]. Specific Toroidal Alfvén Eigenmode (TAE) studies have been carried out [6] by exciting these modes using either in-vessel saddle coils or ICRF beat waves created by energising two antennas with a precisely controlled frequency difference. A new and entirely digital real time plasma position and shape control system [7] has been implemented providing greatly increased flexibility and accuracy. The JET control and data acquisition system is based on a network of dedicated minicomputers (in UNIX environment) which provide centralised control, monitoring and data acquisition on CAMAC and VME standards.

The support of the Vacuum Vessel has been fitted with hydraulic restraints in order to limit vessel displacements, in particular with regard to large sideways forces [8]. New instrumentation is available for measuring halo currents, forces applied to the vessel and the corresponding displacements.

Long pulse operation and scenario optimisation rely on the continuous development of the non-inductive current drive capability of JET which is based mainly on the LHCD system (3 MA has been driven) but also on the fast waves launched from the phased 4-strap ICRH antennas and the quasi-tangential neutral beam lines.

2. DIVERTOR PHYSICS ASPECTS

2.1 JET divertor configurations

X-point tiles fixed directly to the vacuum vessel were used in 1989-91 for H-mode studies in which the target to X-point distance was very small (< 10 cm). As a result, the screening effect of the divertor was mediocre at low divertor densities and a fraction of the impurity atoms sputtered from the target plates could go directly into the main plasma. Furthermore, the divertor plasma was not fully opaque to impurity and hydrogenic neutrals. This was partly beneficial since neutrals could re-enter the SOL well upstream and increase the flow over a significant part of the SOL [2]. However, these neutrals also led to increased impurity influxes by charge exchanged neutral sputtering. The duration of high performance discharges was often limited, ultimately, by a strong influx of carbon impurities, the so-called "carbon bloom". Energies of only about 15 MJ could be conducted to the target plates.

The relatively open Mk I divertor and in-vessel cryopump were installed for JET operation during 1994-95 (Fig.1). For high power handling, the magnetic configuration was swept (4 Hz) horizontally with the help of the in-vessel divertor coils. This allowed energies in excess of 180 MJ (CFC-tiles) and 120 MJ (beryllium tiles) to be conducted to the tiles without significant sublimation or melting occurring [2]. The carbon blooms which previously terminated high performance discharges were avoided. Operation with plasma currents up to 6 MA was possible, the plasma stored energy reached 13.5 MJ and the maximum D-D neutron rate was 4.7×10^{16}/s. A range of divertor physics experiments was conducted with high power (up to 32 MW) and steady-state H-mode plasmas with a radiative divertor using N_2 as the seeded impurity were studied.

The Mk IIA divertor presently used in JET is a moderately closed divertor consisting of a continuous water-cooled divertor structure about 6 m in diameter and weighing about 7 tonnes. It was installed to an alignment accuracy of 1 mm and its replacement is compatible with remote handling. The increased wetted area leads to a power handling capability which is a factor of 3 - 5 better than Mk I. Operation is carried out on both the horizontal and vertical target plates, permitting a comparison of results on impurity retention and neutral recycling, and on the orientation of the target plates both with and without pumping

provided by the cryogenic pump. An extensive experimental campaign has been carried out with this divertor with plasma currents up to 5 MA and energies up to 150 MJ have been accommodated by Mk IIA without producing excessive impurity influxes. A number of configurations such as Standard Fat, Super Fat, High Flux Expansion, Vertical Plate and High X-point (to simulate Gas-Box type) configurations have been used with low (0.18) and high (0.32) triangularity plasmas.

2.2 Regimes of divertor operation

2.2.1 The low recycling regime is characterised by a low temperature gradient (target-upstream), reduced particle flows to the target and low density in the divertor and is required by scenarios providing the highest fusion performance (albeit transiently). The performance increases as the duration of the ELM-free period is increased by reducing the recycling (extensive wall conditioning, use of the cryopump, and use of target plate material such as beryllium and/or beryllium evaporation).

2.2.2 The high recycling regime is characterised by a high density at the target and a high parallel flow of ions to the target helps to retain impurities in the divertor by friction. The radiated power fraction is moderate and it is mostly confined to a narrow region close to the target. This could lead to a high power density at the target and excessive erosion. ITER has therefore also considered a "gas box" design [9] in which the radiation losses in the divertor are enhanced and the exhaust power is distributed over a larger sidewall area of a deep divertor via charge exchange and radiation losses. The target geometry is tailored to enhance this effect and the divertor is relatively closed. Hydrogenic and impurity neutrals are required to recirculate within the divertor region and the loss of these neutrals to the main chamber is minimised with the help of the divertor cryopump. However, flows from the main plasma to the X-point are reduced and this may adversely affect impurity control.

Code calculations at JET and elsewhere show that hydrogenic plasmas cannot radiate sufficiently for the plasma to be extinguished before reaching the target. To achieve this "fully detached" regime, in which the energy reaching the target is negligible, impurity seeding is needed to increase the radiative losses. In experiments at JET with Mk I and Mk IIA, detached plasmas obtained by seeding N_2 in the divertor region have been obtained with up to 80 % of the power being radiated [10]. The plasma then becomes detached as evidenced from the ion saturation current characteristics measured by Langmuir probes in the divertor region. The plasma remains stable, but the continued increase in radiation causes the radiation peak to move from the target plates to the X-point and leads ultimately to a radiative collapse in which the whole plasma surface radiates.

2.3 Differences in performance of Mk I and Mk IIA

2.3.1 Detachment is defined to occur when the ion flux (ion saturation current measured by Langmuir probes) to the target starts to decrease when the density is increased by gas fuelling. In agreement with code calculations, it is found [11] that detachment in L-mode occurs at a factor of 2 lower density in Mk IIA than in Mk I because the increased closure in Mk IIA permits a higher divertor density for the same mid-plane density. H-mode data has not been obtained as the probe characteristics are strongly perturbed by the ELMs.

2.3.2 Neutral particle compression. The loss of hydrogenic and impurity neutrals from the divertor into the main chamber increases the neutral pressure in the main chamber and adversely affects the H-mode power threshold, deteriorates H-mode confinement, and increases the release of impurities from the main

chamber walls by charge exchanged neutral sputtering. Neutral particle retention in the divertor (or closure of the divertor) is important and is generally expressed as a compression ratio between the neutral particle fluxes in the divertor and the main chamber using calibrated hot-ion cathode gauges and D_α measurements. It is found that the compression ratio is higher by a factor of 2 - 2.5 in Mk IIA than Mk I. Particle removal with the cryopump is similarly increased. This result has been confirmed by the measurement of the decay time of injected Neon which is found to be a factor 2 to 4 greater in Mk I (Fig.3).

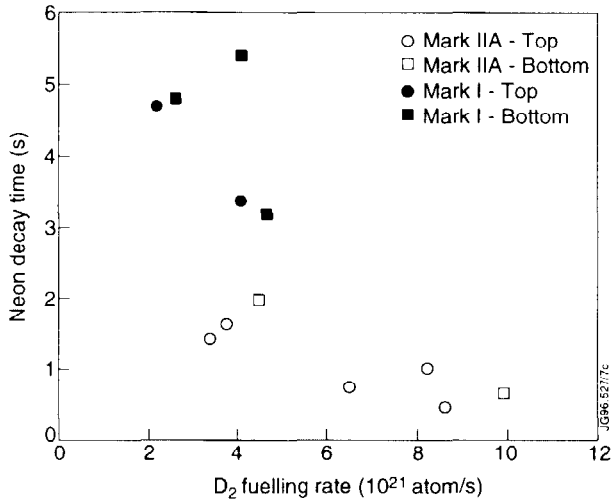

Fig. 3 A comparison of neon decay time as a function of D_2 fuelling rate in Mk I and Mk IIA divertor in neon puff experiments. Top and bottom refer to D_2 fuelling in the main chamber and in divertor respectively.

2.4 Modelling

The multifluid plasma code EDGE2D/U coupled to the Monte Carlo neutral particle code NIMBUS has been used at JET to simulate and compare the modelled and experimentally measured divertor performance. The codes calculate the distribution of deuterium and impurity density, temperature and flow, and other quantities corresponding to measurements such as the ion saturation current density (measured by probes at the divertor target), D_α and bremsstrahlung radiation signals, and the impurity and deuterium radiation power densities. The basic equations include classical (collisional) parallel (along the magnetic field lines) plasma transport for electrons, hydrogenic and impurity ions. Anomalous transport across the field lines is described by a simple prescription in which the transport coefficients are specified and generally taken constant across the SOL. The modelling of divertor plasmas has made good progress during the last few years, but there is still no satisfactory modelling of ELMy H-mode plasmas. The difficulty arises principally from the very large variations in density during and after an ELM and in periods between ELMs. Although between ELMs, the magnetic geometry is well defined, it can be strongly perturbed during the ELM itself. Modelling of long ELM-free H-modes as well as grassy ELMs in radiative H-mode plasmas has been successful since the variation in plasma parameters does not change appreciably on the short time scale.

Generally the modelling of tokamak plasmas treats the edge and core plasma separately, which often leads to artificial boundary conditions between the two regions. At JET, the transport codes describing the plasma core (JETTO) and the plasma edge (EDGE2D/U-NIMBUS) have been coupled using transport

coefficients and fluxes which allow self-consistent modelling [12]. A pinch term is found to be required in the edge transport to simulate the observed narrow SOL. This has allowed an ELM-free hot-ion H-mode to be modelled self-consistently and the results are given in Fig.4.

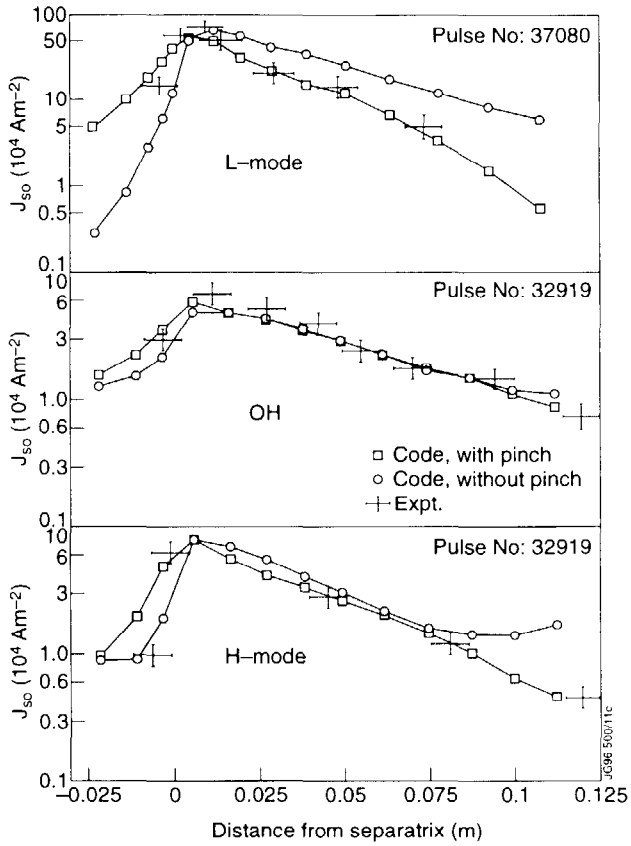

Fig.4 Measured ion saturation current density versus distance from the separatrix in the Mk IIA divertor in L-mode, OH and H-mode discharges is compared with code calculations with and without a pinch term.

An example of a JET L-mode discharge modelled with EDGE2D/U-NIMBUS is shown in Fig.5 [13]. The electron temperature and pressure drop is reproduced by the calculations which include radiation losses in the divertor and SOL.

3. CONFINEMENT ISSUES

3.1 ITER similarity experiments

The prediction of energy confinement in ITER is based on a confinement scaling (ITERH93-P) derived from a multi-machine data base of H-mode discharges. There is a need to confirm this scaling and improve its accuracy by conducting experiments in which dimensionless parameters describing the plasma are varied around ITER values. The most relevant variables are (i) normalised Larmor radius ρ^*, (ii) normalised collisionality ν^* and (iii) normalised plasma pressure β. The ITERH93-P scaling has been written in the dimensionless form as follows [14]:

$$B\,\tau_{ITERH93\text{-}P} \propto \rho^{*\,-2.7}\,\nu^{*\,-0.28}\,\beta^{-1.2} \qquad (1)$$

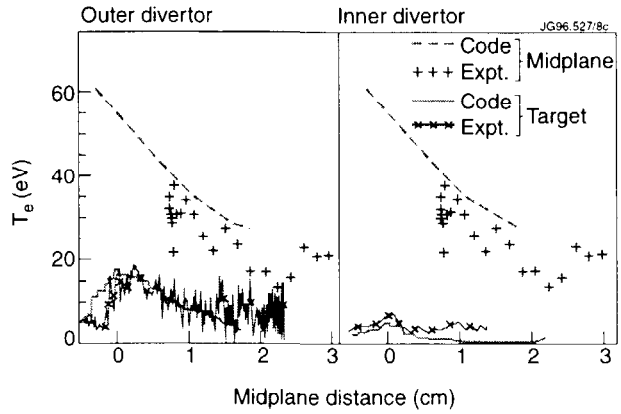

Fig.5 Measured and code calculated electron temperature profiles in the mid-plane and the divertor target for the inner and outer legs of the divertor in an L-mode discharge as a function of distance from the separatrix at the outer mid-plane.

where the parameters ρ^*, ν^* and β are defined in terms of their average values. Recently, careful experiments have been carried out in JET in which each of the three parameters was changed while keeping the other two fixed. Moreover, the power level was significantly above the H-mode threshold and producing type I discrete ELMs. It is concluded (Fig.6) that the dependence on ρ^* (close to gyro-Bohm) and ν^* is correctly described in the ITERH93-P scaling but the dependence on β is found to be very weak ie $\beta^{-0.05}$. It is suspected that the ITERH93-P scaling is based on data which includes some taken too close to the MHD β-limit. This new result on β scaling is more favourable and, if confirmed by other experiments, would increase the ITER confinement at ignition by 10 to 15 %.

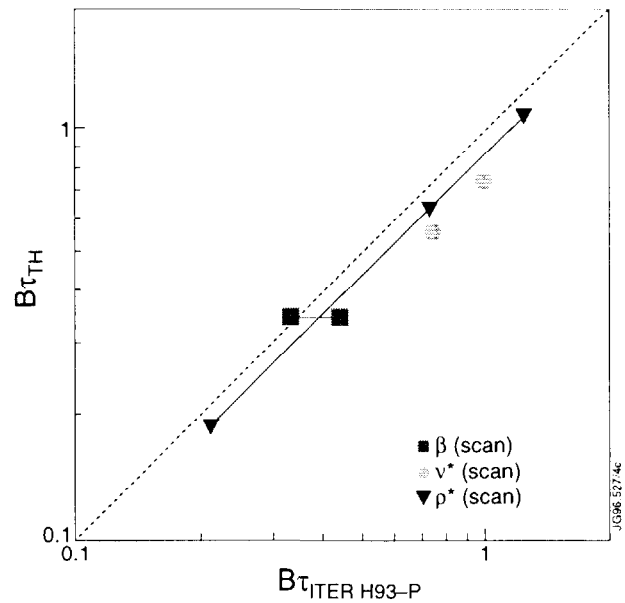

Fig.6 Normalised confinement time $B\,\tau_{th}$ is plotted as a function of $B\,\tau_{ITERH93\text{-}P}$ scaling for ρ^*, ν^* and β-scans. B represents the cyclotron frequency.

3.2 H-mode threshold

Existing H-mode threshold scalings have large data dispersion leading to uncertainty in the threshold: P_{th} = 50 - 200 MW in ITER at a density of

5 x 10^{19} m^{-3}. As the power threshold decreases with density, it is considered to enter the H-mode at low density (2-3 x 10^{19} m^{-3}) and then to increase the density progressively as the α-particle heating increases. The input power has to be somewhat higher than the power threshold, otherwise the confinement is insufficient. ITER ignition scenarios also depend on a possible hysteresis between H to L and L to H transitions. Although there is evidence of hysteresis in ELM-free H-modes, more recent experiments in JET [14] in ELMy H-modes indicate that there is essentially no hysteresis. This behaviour might be different in JET because of the high temperature walls and high pumping which are very effective at controlling recycling. The data on threshold power in Mk IIA can be described by $P_{th} \sim 0.3\ n_{20}\ B\ R^{2.5}$ (x 10^{20} m^{-3} T $m^{2.5}$) but data dispersion is still large, indicating that other aspects will have to be included for an appropriate description of the scaling. The threshold power was found to be independent of the type of additional heating (NBI or ICRH).

3.3 Effect of plasma configuration

The ELM behaviour in JET depends on plasma shape (triangularity), divertor magnetic configuration (high or low flux expansion), neutral recycling in the divertor and in the main chamber, and gas fuelling at the edge. High flux expansion with high triangularity, low recycling and no edge fuelling produces long ELM-free periods during which the confinement time increases continuously to 1.2 - 1.5 times ITERH93-P scaling. Figure 7 shows that, in steady-state discharges with constant power and fuelling, the ELM frequency decreases with increasing triangularity; on the other hand, the energy confinement appears to be independent of triangularity [11].

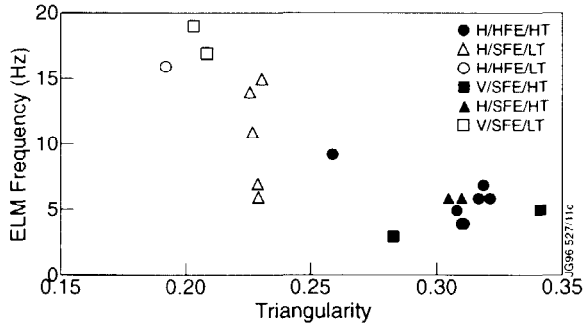

Fig.7 ELM frequency versus plasma triangularity for 2.5 MA, 2.5 T discharges with 12 MW beam power. The notation for the plasma equilibria A/B/C indicates target orientation (H = horizontal, V = vertical), flux expansion (HFE = high, SFE = standard) and triangularity (HT = high, LT = low) respectively.

3.4 Highly radiative ELMy H-modes

Highly radiative plasmas reduce the heat load to the divertor target plates avoiding excessive erosion of the target. An example of a highly radiative divertor discharge [2] which was heated at a power level of 32 MW (17 MW of NBI and 15 MW of ICRH) is shown in Fig.8. Such a discharge was obtained by nitrogen injection to enhance radiation and indeed the radiated power fraction reached 70 % of the total input power. The density reaches steady-state and the H-mode quality factor relative to ITER89-P scaling is about 1.5.

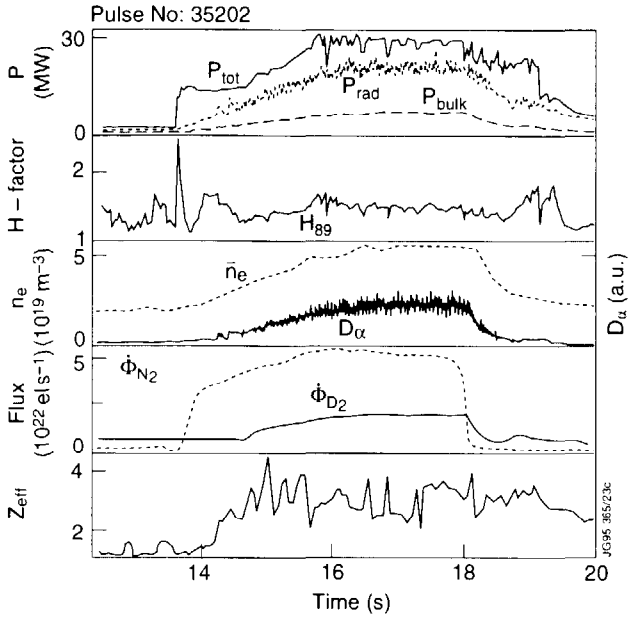

Fig.8 Time traces of an H-mode discharge with 30 MW of combined ICRF and NB heating and more than 70 % of the power is exhausted by radiation from seeded nitrogen.

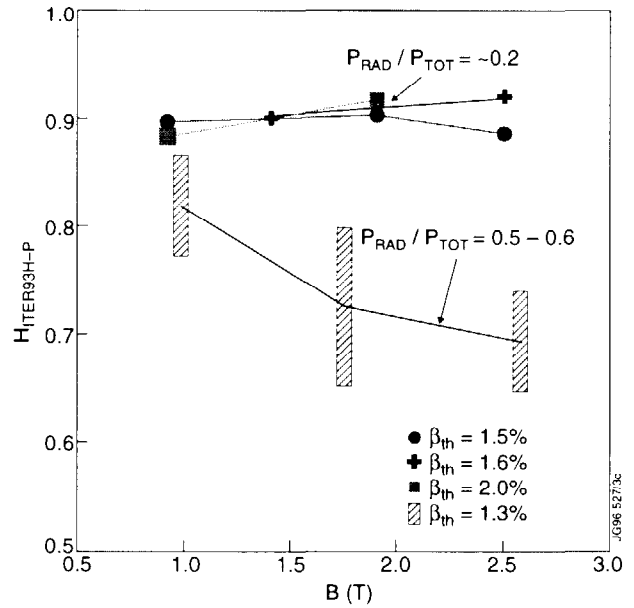

Fig.9 Confinement (normalised to ITERH93-P) versus toroidal field B in discharges with low and high radiated power fractions. Confinement degrades with radiation and loses gyro-Bohm scaling.

The confinement quality degrades progressively with increasing radiation and impurity concentrations in the main plasma can be high if the plasma density is too low. When the radiated power fraction is larger than 0.5, the confinement scaling is seen to become worse than gyro-Bohm scaling (Fig.9, [15]). A multi-machine size scaling for Z_{eff} in radiating divertor plasmas has been established so that a value for ITER can be predicted. The data from various divertor tokamaks

world-wide is included with the proviso that discharges have a radiated power fraction larger than 50 %. The following scaling best represents the data [16]:

$$Z_{eff} = 1 + 5.6\ P_R\ Z^{0.19} / (< n_e >^{1.95}\ S^{1.03}) \qquad (2)$$

where P_R (MW) is the radiated power, S (m^2) is the plasma surface area, $< n_e >$ (10^{20} m^{-3}) is the line averaged density and Z is the atomic number of the seeded impurity. The Z_{eff} data obtained with the Mk I and Mk IIA divertors of JET are plotted as a function of this scaling as shown in Fig.10. The value of Z_{eff} predicted for ITER in such highly radiating discharges (85 %) and $< n_e > = 1.2 \times 10^{20}$ m^{-3} would be about 1.6. According to this scaling, ITER would have a tolerable impurity level. There is a clear need to increase the data set with data obtained in other divertor configurations.

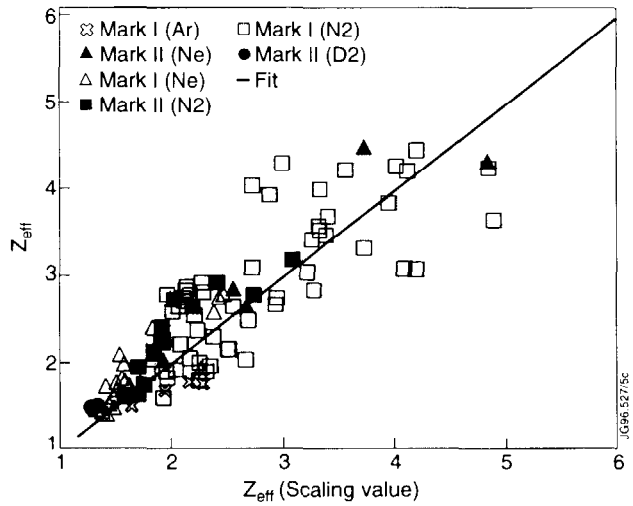

Fig.10 Measured effective charge (Z_{eff}) versus the scaling of Eq.(2) for a number of JET discharges in Mk I and Mk IIA with seeded impurity gas as indicated. The solid line is a fit to the data.

4. ENERGETIC PARTICLE EFFECTS

Alpha particles will be the dominant power source in ITER. Therefore, the confinement of the energetic α-particles and the impact on plasma performance are important issues. Moreover, any uncontrolled loss of α-particles either by collective instabilities such as Toroidal Alfvén Eigenmodes (TAE) or ripple induced losses could have serious consequences for the first wall.

4.1 TAE excitation

Global Alfvén eigenmodes can be excited by energetic particles such as fusion born α-particles, injected neutral beam ions or fast-ions accelerated by ICRH. In a reactor, the destabilisation of these modes can lead to a spatial redistribution or an enhanced loss of α-particles with the result that they may not fully heat the plasma. There are a variety of effects which can dampen the modes and both the driving and damping effects must be evaluated to assess the linear stability. External excitation of the modes has been done in two ways: (i) by saddle-coils mounted inside the vacuum vessel and (ii) by beat waves generated by two ICRH antennas run master-slave at slightly different frequencies (100 - 200 kHz at 50 MHz). A coherent detection of AEs in the magnetic, electron cyclotron emission or reflectometry diagnostics provides a means of determining

their damping rates. Measurements are made in the presence of a varying fast particle drive, such as 140 keV deuterium NBI, in order to resolve the differences in damping and driving rates of the mode. A feedback loop acting on the frequency of the exciter is used to track chosen eigenmodes during the discharge. Figure 11 shows such a real-time tracking of AEs [17] over a period of 2.5 s in which the frequency of the exciter oscillates around the mode frequency and provides a means of determining the damping rate as a function of time. Values of $\gamma / \omega = 0.55$ - 0.59 % are found, compared to the theoretical estimates of about 1 %. The application of high power NB heating appears first to dampen the n = 1 mode but later the phase resolved measurements by several MHD coils indicate that higher order modes up to n = ±20 start to grow at the AE frequency. These modes are routinely observed during hot ion H-modes with 140 keV NBI with $V_{||} = V_A / 3$ and could be responsible for limiting the fusion performance. Kinetic TAEs have been identified. Ballooning AEs have also been observed.

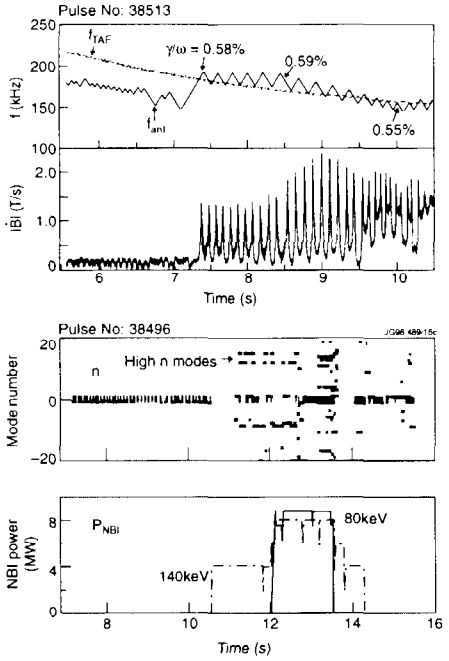

Fig.11 Tracking during the ohmic phase of TAEs (n = 1) excited by the saddle coils and high-n modes driven unstable at $V_A/3$ by high power 140 keV NB heating.

4.2 Confinement of fast ions

Ion cyclotron minority heating has been used previously in JET to produce 1 - 1.5 MeV He^3 ions with an energy content up to 2 - 2.5 MJ corresponding to almost 40 - 50 % of the total plasma energy of such discharges [18]. The suprathermal ion energy could be described by classical slowing down of the fast ions. Further studies have been carried out of central ICRF heating at the third harmonic of deuterium in JET where suprathermal effects are dominant and a very energetic tail is expected to develop that does not cut off until 4 MeV when the ion orbits reach the limiters. The deuterium neutron rate in these discharges is observed to reach a high value of 9 x 10^{15}/s due to the energetic deuterium tail. These results were well reproduced by PION code calculations, giving confidence in the understanding of the production and confinement of energetic tails [19].

4.3 Ripple experiments

The effect of toroidal field ripple on plasma behaviour and fast particle losses was studied with the Mk I divertor. The ripple was varied in the ITER relevant range of 0.1 to 2 %. Ripple induced losses of thermal and high energy particles (125 keV neutral beam ions and 1 MeV tritons) were less than 1 % and were consistent with theoretical estimates. However, the observed losses of particles of intermediate energy (thermal to tens of keV) were higher than predicted [2]. The slowing down of rotation due to ripple was also a notable result of these experiments.

5. HIGH PERFORMANCE AND STEADY STATE REGIMES

In preparing for the D/T phase, JET is pursuing two scenarios for high fusion performance: (i) hot-ion H-mode and (ii) optimised shear mode. Good fusion performance is also achieved in steady-state at high current (5 MA) in a regime directly relevant to ITER.

5.1 Hot ion H-mode

Traditionally "hot ion H-mode" refers to operation with strong neutral beam heating of a low electron density target plasma, with high triangularity (0.25) and high flux expansion in the divertor. Central NB power deposition and central fuelling produces a moderately peaked density profile. The neutral beam predominantly heats the ions and T_i exceeds T_e considerably (> 2 - 2.5) over the inner half of the plasma radius. The high performance lasts for about 2 s and is terminated either brutally or softly ("roll over") by a complex and largely unexplained event [20] involving (i) sawteeth or other internal MHD phenomena occurring in the central region, (ii) "outer-modes" occurring in the body of the plasma and (iii) "giant" ELMs at the plasma edge. The outer modes have now been identified by detailed soft X-ray measurements as ideal kink modes [20] and giant ELMs appear when the ballooning instability criterion is satisfied. The rollover in performance could be linked to the excitation of TAEs (Section 4.1) where the TAE resonance condition $V_{||} = V_A / 3$ for the 140 keV neutral beam is satisfied. Code calculations suggest that, at the resonance condition, sufficient beam ion redistribution within the plasma could account for the degradation in performance.

LHCD has been used to eliminate the sawteeth and to soften the effect of the outer modes but the performance is still limited at a normalised $\beta_N \approx 1.8$ well below the Troyon limit ($\beta_N = 2.8$). More recently, ICRH has been applied to hot ion H-modes [21]. The effect of the ICRH is shown in Fig.12. The addition of 6 MW of ICRH improves the rate of rise of the neutron rate, increases the stored energy by about 5 MJ and T_e by about 30 %. Therefore good confinement is maintained even when the power input to the electrons is substantially increased. A stored energy of up to 14 MJ was obtained with combined heating. Power step-down experiments allow the highest Q to be reached.

5.2 Discharges with optimised shear

Weak or reversed magnetic shear has been associated with improved core confinement since the JET experiments with deep pellet injection (PEP mode [22]). MHD instabilities like ballooning, resistive tearing and internal MHD modes are then stabilised provided that low rational values of q are avoided. Shear of plasma rotation (plasma flows) has also been shown by theory to stabilise microinstabilities involved in anomalous transport. In such a situation, an internal transport barrier can be established and the resulting steep ion temperature gradient produces more rotation shear.

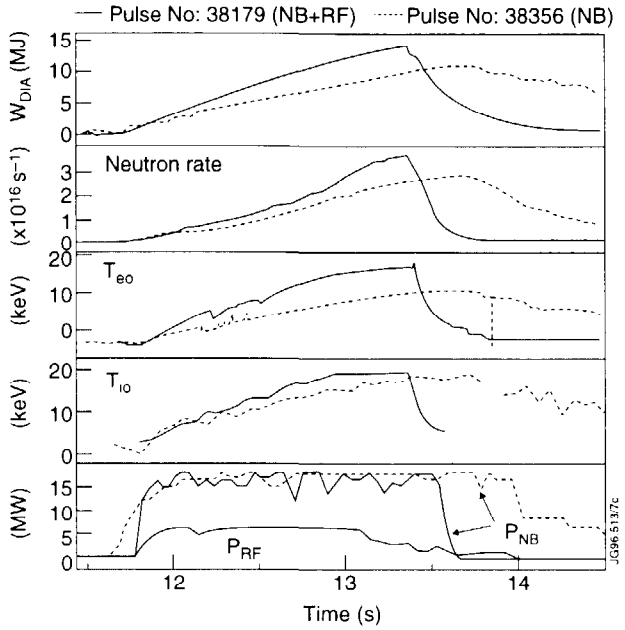

Fig.12 Time traces of NB heated hot ion H-modes with and without ICRH.

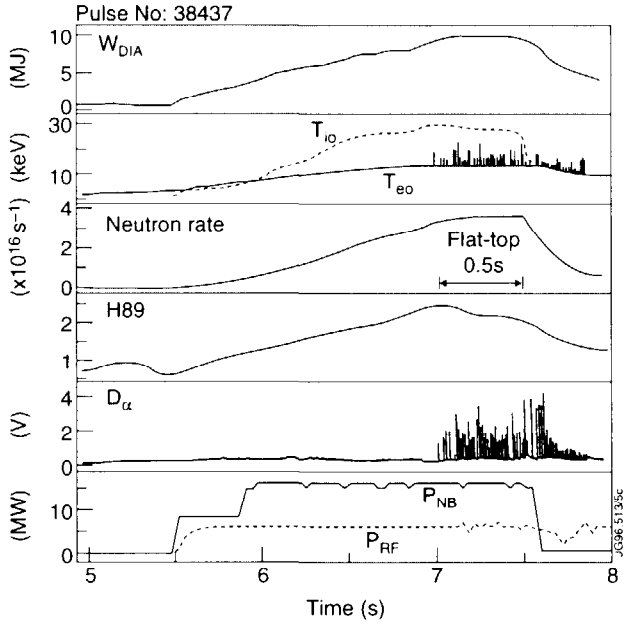

Fig.13 Time traces of a combined (NB + ICRF) heating optimised shear discharge giving enhanced core confinement. H89 refers to an improvement of confinement over the ITER89-P (L-mode) scaling.

In JET, optimised shear experiments [23] are carried out immediately after the current rise phase of the discharge where advantage is taken of the natural delay in the current diffusion to the plasma centre as the current is ramped up. The current diffusion can be further delayed by electron heating by ICRH. The target plasma has q > 1 everywhere. Neutral beams and ICRH are injected at optimised times in the low target plasma density. An example of time traces of such a high performance discharge is shown in Fig.13 where the maximum

neutron rate of 3.4 x 10^{16} /s is flat for ~ 0.5 s, the stored energy is 9.4 MJ and the peak T_e and T_i are 14 keV and 28 keV respectively. The q profile obtained from a combination of EFIT equilibrium code and Faraday rotation measurements shows that the magnetic shear in the core is weak and slightly positive just before and during the heating. Figures 14 and 15 compare the profiles of T_i, pressure P and rotation ω in the above two high performance modes. The internal confinement barrier corresponds to r/a ~ 0.55. The shear in plasma rotation is large at this location.

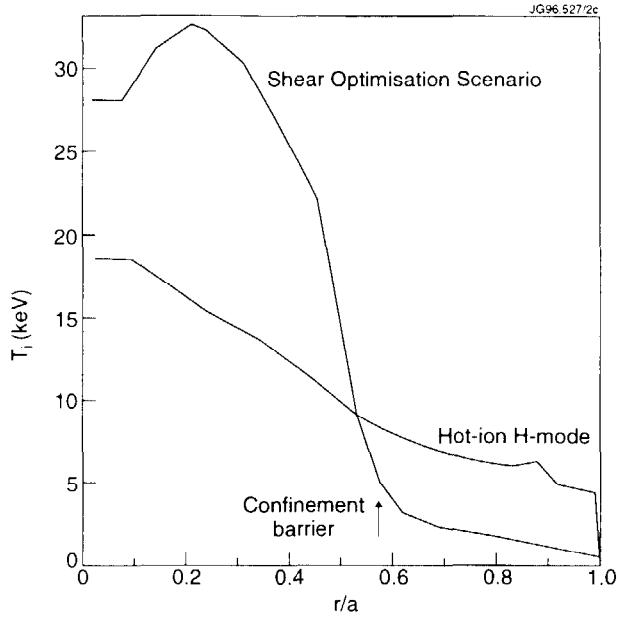

Fig.14 A comparison of typical ion temperature profiles in a hot ion H-mode and an optimised shear discharge.

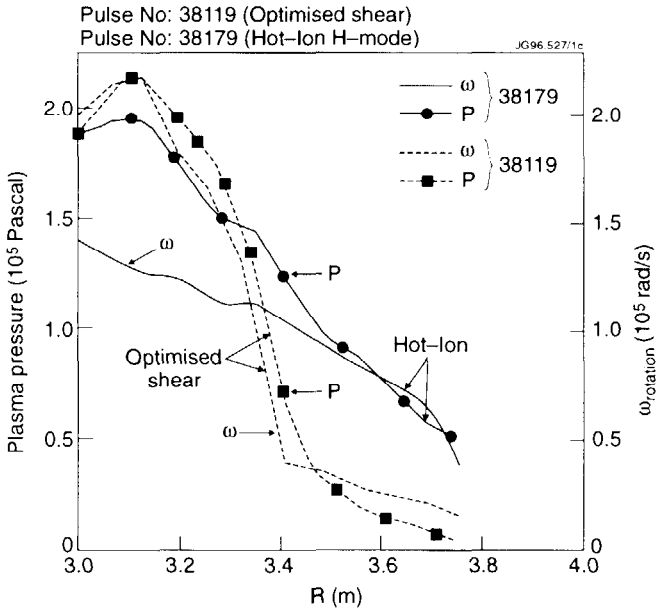

Fig.15 Profiles of total plasma pressure and poloidal rotation frequency in a hot ion H-mode and an optimised shear discharge.

5.3 High current plasmas and approach to steady-state

The combined advantages of the high power handling of Mk IIA, the divertor cryopump and the high recycling conditions established in the divertor enable the production of long pulse steady-state H-modes. ELMy H-modes of 20s duration at 2 MA were achieved in Mk I [24]. Recently, this regime has been extended to higher plasma currents (4.7 MA) and higher input powers with combined ICRH and NB heating. An example of a discharge at 4.7 MA is given in Fig.16 where a fusion triple product of 4 x 10^{20} (m^{-3} s keV) is maintained for 1.5s. This constitutes substantial progress from the best steady-state performance presented [24] at the 1994 IAEA Conference (2.65 x 10^{20} m^{-3} s keV). At higher power (28 MW), the plasma stored energy reached a new world record of 15 MJ. However, steady-state was not achieved in this case. The reasons for this are not clear. It should be noted that in these high current discharges the plasma density increases over several seconds and it is more difficult to maintain the input power above the H-mode power threshold.

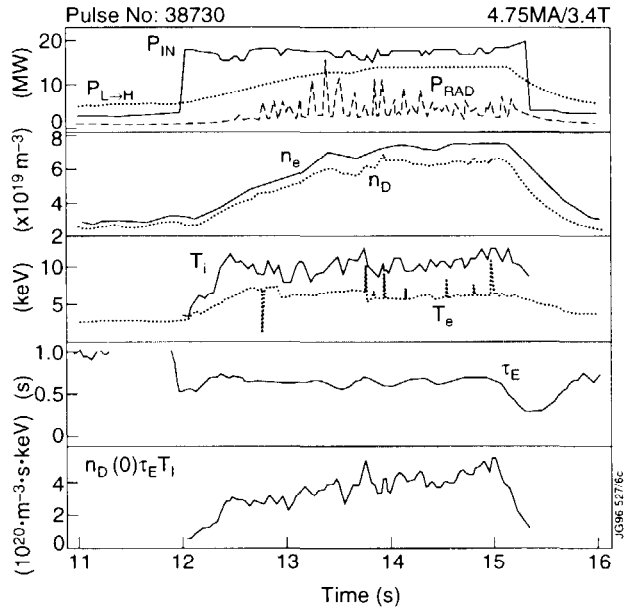

Fig.16 Time traces of a high power 4.7 MA discharge where the fusion triple product reaches a value of 4 x 10^{20} m^{-3} s keV. $P_{L\rightarrow H} \propto nBS$ represents an L- to H-mode threshold power scaling.

6. JET FUTURE PROGRAMME

In the present Mk IIA configuration the conductance of the "by-pass leak" between the divertor and the main torus chamber is comparable to the pumping rate of the cryopumps. These leaks reduce the neutral pressure in the divertor and increase it in the main chamber. They could contribute to the pollution of the main plasma and adversely affect the evaluation of the divertor performance such as the effect of pumping, gas fuelling at different locations within the divertor and seeding of N_2 impurity. The conductance will be reduced by a factor of 5 after a machine intervention in October 1996 to close the larger gaps.

Another divertor configuration is scheduled to be investigated in JET during 1997/98: the so-called Gas Box configuration which will simulate the presently chosen configuration for ITER. It has a large open region close to the target and a narrower entrance. The X-point is high to achieve the longest

divertor leg length adjacent to the region of free recirculation of neutrals from the target while minimising the escape of neutrals to the main chamber. Operation with Mk II GB would emphasise the divertor SOL plasma being extinguished (detached) before the target plates are reached. The target configuration can be changed from vertical to horizontal targets by removing parts of the tiles. The target tiles and the tile carriers are both fabricated from CFC and will be installed in JET by remote handling just after the DTE1 experiments.

D/T operation (DTE1) is planned to start on JET in early 1997. The effect of tritium on energy confinement and H-mode threshold will be assessed for the first time in an ITER-like divertor configuration. These experiments are also aimed at demonstrating long-pulse fusion power production with expected fusion power output in the range of 10 MW for several confinement times. A second period of high performance D/T operation (DTE2) is scheduled to take place in 1999. It will take advantage of a preceding period for optimising the operating modes and the in-vessel configuration. This period of D/T operation will also provide a full scale test of the technology of processing tritium in conjunction with an operating tokamak and the experiments will address α-particle heating and associated effects.

7. DISCUSSION AND CONCLUSIONS

JET has conducted a wide range of experiments in both an open and moderately closed divertor configuration. The issues of confinement quality, plasma purity and divertor operating conditions have been addressed and are reported in ten papers at this Conference. The excellent power handling of the Mk IIA divertor has been demonstrated and has allowed new performance developments including a record plasma energy of 15 MJ and a high fusion triple product in high current steady-state discharges.

Modelling of the particle and power exhaust in the divertor has progressed and describes the observations well, with the notable exception of discharges with large ELMs which are not presently taken into account accurately.

Long pulse ITER dimensionless conditions and type I ELMs satisfy the ITER confinement requirements. The ITERH93-P confinement scaling is confirmed over a broad range of parameters but the scaling with β is found to be more favourable. If this is confirmed on other experiments, the confinement time predicted for ITER should increase by about 10 to 15 %.

Confinement degrades in highly radiating discharges and Z_{eff} can be large in impurity seeded discharges at low density. Plasma purity is better at high density and a data base quantifies the expected plasma purity in ITER.

In addition to the hot ion H-mode, a second high performance regime has been developed in JET. It is based on optimising the plasma current profile. With low central magnetic shear and $q > 1$ everywhere in the plasma, internal confinement barriers are observed above a power threshold which is presently about 17 MW. This regime appears similar to that obtained with identical geometry in DIII-D. It is significant that the confinement barrier appears in JET despite a lower fuelling and toroidal momentum input in JET than in DIII-D.

D/T experiments will start in early 1997. The experiment will address the effect of tritium on energy confinement and H-mode threshold in an ITER-like divertor configuration.

ACKNOWLEDGEMENTS

The JET team wishes to acknowledge the collaborations with the European Institutions which were essential to the progress made throughout this research. The optimised shear experiments reported here were conducted in collaboration

with the DIII-D team (General Atomics, USA). The author wishes to thank Dr V Bhatnagar for the preparation and editing of this paper.

REFERENCES

[1] JET TEAM (presented by P.H. Rebut), in Plasma Physics and Controlled Fusion Research 1990 (Proc. 13th Int. Conf. Washington, 1990), Vol. 1, IAEA, Vienna (1991) 27.
[2] JET TEAM, Plasma Phys. Control. Fusion **37** (1995) A3.
[3] JET TEAM, Nucl. Fusion **32** (1992) 187.
[4] VLASES, G.C. and SIMONINI, R., in Controlled Fusion and Plasma Physics (Proc. 18th Eur. Conf. Berlin, 1991) Vol. 15C, part III, European Physical Society, Geneva (1991) 221.
[5] STOTT, P., paper presented at Fusion Technology 1996 (Proc. 19th Symp. (SOFT), Lisbon, 1996).
[6] FASOLI, A. et al., Nucl. Fusion **35** (1995) 1485.
[7] PUPPIN, S. et al., paper presented at Fusion Technology 1996 (Proc. 19th Symp. (SOFT), Lisbon, 1996).
[8] JET TEAM (presented by A. Tanga), IAEA-CN-64/AP1-18, this Conference.
[9] REBUT, P.H. et al., Fusion Eng. and Design **22** (1993) 7.
[10] JET TEAM, Plasma Phys. Control. Fusion **37** (1995) A227.
[11] JET TEAM (presented by G. Vlases), IAEA-CN-64/A4-1, this Conference.
[12] JET TEAM (presented by A. Taroni), IAEA-CN-64/D3-3, ibid.
[13] LOARTE, A., paper presented at 12th Int. Conf. on Plasma Surface Interactions, St. Raphael, France, 1996 (to be published in J. Nucl. Mater.).
[14] JET TEAM (presented by J.G. Cordey), IAEA-CN-64/A2-1, this Conference.
[15] JET TEAM (presented by D. Stork), IAEA-CN-64/A1-1, ibid.
[16] MATTHEWS, G.F. et al., paper presented at 12th Int. Conf. on Plasma Surface Interactions, St. Raphael, France, 1996 (to be published in J. Nucl. Mater.).
[17] JET TEAM (presented by D.F.H. Start), IAEA-CN-64/A2-6, this Conference.
[18] JACQUINOT, J. et al., Fusion Technology **21** (1992) 2254.
[19] N'GUYEN, F. et al., in Controlled Fusion and Plasma Physics (Proc. 22nd Eur. Conf. Bournemouth, 1995) Vol. 19C, part II, European Physical Society, Geneva (1995) 353.
[20] JET TEAM (presented by P.R. Thomas), IAEA-CN-64/A3-2, this Conference.
[21] JET TEAM (presented by P. Lomas), IAEA-CN-64/A1-5, ibid.
[22] HUGON, M. et al., Nucl. Fusion **32** (1992) 33.
[23] JET TEAM (presented by C. Gormezano), IAEA-CN-64/A5-5, this Conference.
[24] JET TEAM (presented by D. Stork), in Plasma Physics and Controlled Fusion Research 1994 (Proc. 15th Int. Conf. Seville, 1994), Vol. 1, IAEA, Vienna (1995) 51.

Appendix I

THE JET TEAM

JET Joint Undertaking, Abingdon, Oxon, OX14 3EA, U.K.

J.M. Adams[1], P. Ageladarakis, S.Ali-Arshad, B. Alper, H. Altmann, P. Andrew, N. Bainbridge, P. Bak[12], B.Balet, Y. Baranov[8], P. Barker, R. Barnsley[2], M. Baronian, K. Barth, D.V. Bartlett, A.C. Bell, E. Bertolini, V. Bhatnagar, A.J. Bickley, H. Bindslev, K. Blackler, D. Bond, T. Bonicelli, D. Borba, M. Brandon, P. Breger, H. Brelen, P. Brennan, W.J. Brewerton, M.L. Browne, T. Budd, A. Burt, P. Burton, T. Businaro, M. Buzio, C. Caldwell-Nichols, D.J. Campbell, D. Campling, P. Card, G. Celentano, C.D. Challis, A.V. Chankin, A. Cherubini, D. Chiron, J. Christiansen, P. Chuilon, D. Ciric, R. Claesen, H.E. Clarke, S. Clement, J.P. Coad, U. Cocilovo[10], I. Coffey[7], G. Conway[17], S. Cooper, J.G. Cordey, G. Corrigan, G. Cottrell, M. Cox[7], P. Crawley, R. Cusack, N. Davies, S.J. Davies, J.J. Davis, M. de Benedetti, H. de Esch, J. de Haas, E. Deksnis, N, Deliyanakis, E. di Marchi, A. Dines, S.L. Dmitrenko, J. Dobbing, N. Dolgetta, S.E. Dorling, P.G. Doyle, H. Duquenoy, A.M. Edwards[7], A.W. Edwards, J. Egedal, J. Ehrenberg, A. Ekedahl[11], T. Elevant[11], J. Ellis, M. Endler[13], S.K. Erents[7], L.G. Eriksson, H. Falter, J.W. Farthing, A. Fasoli[18], B. Fechner, M. Fichmüller, B. Fischer, G. Fishpool, C. Froger, K. Fullard, M. Gadeberg, L. Galbiati, E. Gauthier[3], R. Giannella, A. Gibson, R.D. Gill, D. Godden, A. Gondhalekar, M. Goniche[5], D. Goodall[7], C. Gormezano, C. Gowers, J. Graham, K. Guenther, R. Guirlet[3], H. Guo[22], A. Haigh, B. Haist[4], C.J. Hancock, P.J. Harbour, N.C. Hawkes[7], N.P. Hawkes[1], J.L. Hemmerich, T. Hender[7], J. Hoekzema, L. Horton, J. How, A. Howman, M. Huart, T.P. Hughes, F. Hurd, G. Huysmans, A. Hwang, C. Ibbott, C. Ingesson[15], B. Ingram, M. Irving, J. Jacquinot, H. Jaeckel, P. Jaeckel, J.F. Jaeger, O.N. Jarvis, F. Jensen, M. Johnson, E.M. Jones, L.P.D.F. Jones, T.T.C. Jones, J-F. Junger, F. Junique, A. Kaye, B.E. Keen, M. Keilhacker, W. Kerner, N.G. Kidd, Q.A. King, S. Knipe, R. Konig, J.G. Krom, H. Kubo[19], P. Kupschus, P. Lamalle[14], R. Lässer, J.R. Last, L. Lauro-Taroni, K. Lawson[7], M. Lennholm, J. Lingertat, A. Loarte, P.J. Lomas, M. Loughlin, T. Lovegrove, C. Lowry, A.C. Maas[15], B. Macklin, C.F. Maggi[16], M. Mantsinen[5], V. Marchese, F. Marcus, J. Mart, D. Martin, T. Martin, G. Matthews, H. McBryan, G. McCormick[13], G. McCracken, P.A. McCullen, A. Meigs, P. Miele, F. Milani, J. Mills, R. Mohanti, R. Monk, P. Morgan, D. Muir, G. Murphy, F. Nave[21], G. Newbert, P. Nielsen, P. Noll, W. Obert, D. O'Brien, E. Oord, R. Ostrom, M. Ottaviani, S. Papastergiou, V.V. Parail, R. Parkinson, W. Parsons, B. Patel, A. Paynter, A. Peacock, N. Peacock[7], R.J.H. Pearce, C. Perry, M.A. Pick, J. Plancoulaine, O. Pogutse, L. Porte, R. Prentice, S. Puppin, G. Radford[9], T. Raimondi, R. Reichle, V. Riccardo, E. Righi, F. Rimini, A. Rolfe, A. Rookes[17], R.T. Ross, A. Rossi, L. Rossi, G. Sadler, G. Saibene, M. Salisbury[12], A. Santagiustina, F. Sartori, R. Sartori, R. Saunders, P. Schild, M. Schmid, V. Schmidt, B. Schokker[15], B. Schunke, M. Scibile, S.M. Scott, S. Sharapov, A. Sibley, R. Simonini, A.C.C. Sips, P. Smeulders, O. Smith[12], P. Smith, R. Smith, F. Söldner, J. Spence, E. Springmann, M. Stamp, P. Stangeby[20], D.F. Start, D. Stork, P.E. Stott, P. Stubberfield, D. Summers, L. Svensson, P. Svensson, A. Tabasso[12], M. Tabellini, J. Tait, A. Tanga, A. Taroni, C. Terella, P.R. Thomas, K. Thomsen, B. Tubbing, Y. Ul'Haq[12], A. Vadgama, P. van Belle, R. van der Linden, G. Vlases, M. von Hellermann, T. Wade, R. Walton, D. Ward, M.L. Watkins, N. Watkins[1], M.J. Watson, J. Wesson, M. Wheatley, D. Wilson, T. Winkel, C. Woodward, D. Young, I.D. Young, Q. Yu[6], F. Zannelli, K-D. Zastrow, W. Zhang[12], N. Zornig, W. Zwingmann.

PERMANENT ADDRESSES

1. UKAEA, Harwell, Didcot, Oxon, UK.
2. University of Leicester, Leicester, UK.
3. CEA, Cadarache, France.
4. KFA, Jülich, Germany.
5. Helsinki University of Technology, Espoo, Finland.
6. Institute of Plasma Physics, Hefei, P R of China.
7. UKAEA Culham Laboratory, Abingdon, Oxon, UK.
8. A.F. Ioffe Institute, St. Petersburg, Russia.
9. Institute of Mathematics, University of Oxford, UK.
10. ENEA, CRE Frascati, Roma, Italy.
11. Royal Institute of Technology, Stockholm, Sweden.
12. Imperial College, University of London, UK.
13. Max Planck Institut für Plasmaphysik, Garching, Germany.
14. Plasma Physics Laboratory, ERM-KMS, Brussels, Belgium.
15. FOM Instituut voor Plasmafysica, Nieuwegein, The Netherlands.
16. Dipartimento di Fisica, University of Milan, Milano, Italy.
17. University of Saskatchewan, Saskatoon, Canada.
18. EPFL, Lausanne, Switzerland.
19. JAERI, Tokyo, Japan.
20. Institute for Aerospace Studies, University of Toronto, Canada.
21. LNETI, Savacem, Portugal.
22. INRS-Energieet Materiaux, Univ. du Quebec, Canada.

At July, 1996